Scaling of capillary trapping in unstable two-phase flow: Application to CO[subscript 2] sequestration in deep saline aquifers

Citation: Szulczewski, Michael L., Luis Cueto-Felgueroso, and Ruben Juanes. "Scaling of Capillary Trapping in Unstable Two-Phase Flow: Application to CO2 Sequestration in Deep Saline Aquifers." Energy Procedia 1, no. 1 (February 2009): 3421–3428. © 2009 Elsevier Ltd.

As Published: http://dx.doi.org/10.1016/j.egypro.2009.02.132

Publisher: Elsevier B.V.

Persistent URL: http://hdl.handle.net/1721.1/96264

Version: Final published version: final published article, as it appeared in a journal, conference proceedings, or other formally published context

Available online at www.sciencedirect.com

ScienceDirect

Energy Procedia 1 (2009) 3421–3428

Energy Procedia

www.elsevier.com/locate/procedia

GHGT-9

Scaling of capillary trapping in unstable two-phase flow: Application to CO_2 sequestration in deep saline aquifers

Michael L. Szulczewski, Luis Cueto-Felgueroso, Ruben Juanes*

Massachusetts Institute of Technology. 77 Massachusetts Avenue, Cambridge, MA 02139, USA

Abstract

The effect of flow instabilities on capillary trapping mechanisms is a major source of uncertainty in CO_2 sequestration in deep saline aquifers. Standard macroscopic models of multiphase flow in porous media are unable to explain and quantitatively predict the onset and structure of viscous-unstable flows, such as the displacement of brine by the injected CO_2. We present the first step of a research effort aimed at the experimental characterization and mathematical (continuum) modeling of such flows. Existing continuum models of multiphase flow are unable to explain why preferential flow (fingering) occurs during infiltration into homogeneous, dry soil. We present a macroscopic model that reproduces the experimentally observed features of fingered flows. The proposed model is derived using a phase-field methodology and does not introduce new independent parameters. From a linear stability analysis, we predict that finger velocity and finger width both increase with infiltration rate, and the predictions are in quantitative agreement with experiments.

Keywords: multiphase flow; CO_2 sequestration; capillary trapping; gravity fingering; phase-field modeling.

1. Introduction

One of the major concerns in any sequestration project is the potential leakage of the CO_2 into the atmosphere. Because the CO_2 is less dense than brine, it tends to migrate upwards to the top of the geologic structure. The success of a sequestration project depends heavily on the mechanism of capillary trapping, by which the CO_2 phase is disconnected into an immobile (trapped) fraction. The application of the present paper is, specifically, the prediction of capillary trapping in geological CO_2 storage projects at the field scale.

We investigate, by means of laboratory experiments, the dependence of capillary trapping on the flow dynamics and, in particular, on the instability of the injected CO_2 plume. Factors that contribute to flow instability (and, thereby, reduced storage efficiency) are viscous fingering, permeability channeling, and gravity override. Here we report the results of laboratory experiments of unstable fluid displacements in a transparent glass-bead pack, which enables simple visualization techniques to monitor the flow. We perform drainage of a low-viscosity fluid followed

* Corresponding author. Tel.: +0-000-000-0000 ; fax: +0-000-000-0000 .
E-mail address: juanes@mit.edu.

doi:10.1016/j.egypro.2009.02.132

by imbibition, at different viscosity ratios, flow rates and tilt angle that span the range of conditions found in geologic CO_2 storage.

The experimental observations and high-resolution numerical simulations can be summarized as follows: the effectiveness of capillary trapping decreases with increasing "disorder" of the injected CO_2 plume. We show that the residual nonwetting-phase saturation measured from core floods is not representative of the average values attained in multidimensional, large-scale flows. We confirm that current field-scale simulation models of CO_2 storage overestimate the amount that is actually trapped, because they do not capture the subgrid variability ("disorder") due to viscous and gravity instabilities, and permeability channeling. The main result of the paper is a correlation between an effective trapping coefficient and storage efficiency.

It is fair to say that current formulations of multiphase flow through porous media are incorrect or, at best, incomplete. All models are based on a straightforward extension of Darcy's law to several flow fluid phases. Such models simply cannot capture some of the essential behavior of fluid-fluid displacement in porous media. Examples of behavior observed in physical experiments and that current models cannot reproduce are: (1) viscous fingering during the injection of a less viscous fluid (water, gas, or solvent) into a more viscous fluid (oil); (2) gravity fingering during oil recovery by gravity drainage. In Figure 3 we show a sequence of two displacements performed in our lab: first drainage, followed by imbibition. The prediction of the residual oil saturation is heavily dependent on the pattern of the initial invasion of the fluid.

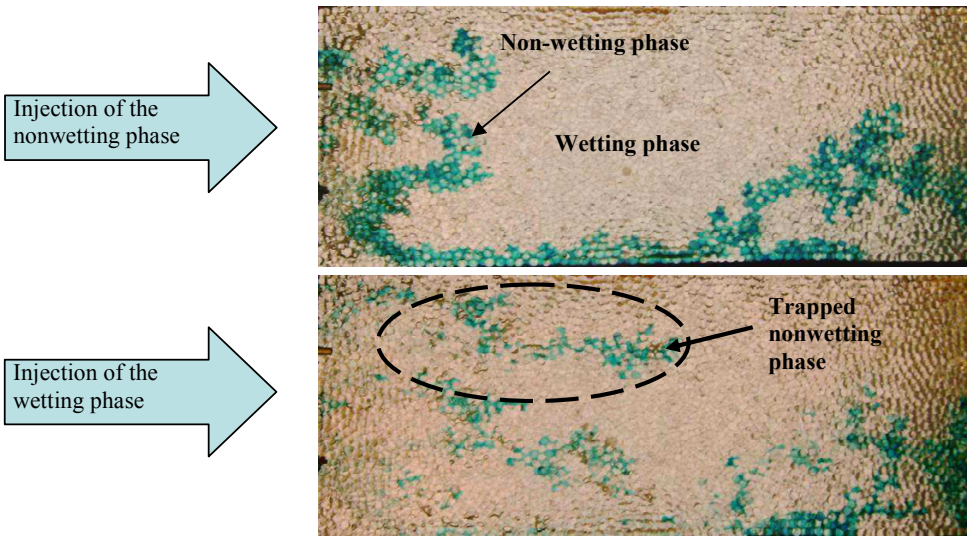

Fig. 1 Unstable displacement of a wetting fluid by a less viscous, non-wetting fluid (drainage), followed by imbibition. These results illustrate the complexity of instable displacements in multiphase flor in porous media, and the dependence of the residual oil saturation on the displacement pattern of the initial drainage displacement.

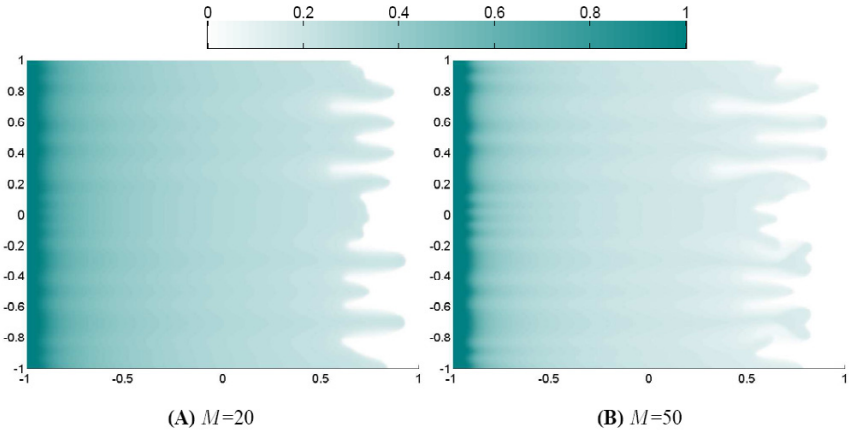

Fig. 2 Numerical simulation of a viscous-unstable displacement using the standard macroscopic theory of flow in porous media. Maps of water saturation at breakthrough time. **(A)** Mobility ratio M= 20, and **(B)** Mobility ratio M= 50.

2. A phase-field model of unsaturated flow through porous media

Existing continuum models of multiphase flow in porous media are unable to explain why preferential flow (fingering) occurs during infiltration into homogeneous, dry soil. Fingering patterns have been consistently observed in laboratory and field experiments for nearly half a century [1,2]. Fingering leads to smaller residence times of contaminants in soil, may play an important role in soil weathering at the time scale of millennia [3], and it may be crucial to the impact of water dropout on the operational efficiency of polymer electrolyte fuel cells [4].

Despite the frequent occurrence of gravity fingers in unsaturated media, the explanation, modeling and prediction of fingered flows with continuum (macroscopic) mathematical models has remained elusive. Many authors have approached the wetting front instability by drawing an analogy with the two-fluid system in a Hele–Shaw cell [5], and their analyses have led to kinematic models that reproduce trends observed in the experiments, such as relations between finger width and finger tip velocity with the flow rate through the finger [2,6-9]. Simulation of unstable gravity flows has also been performed with modified invasion-percolation models at the pore scale [10,11].

By contrast, conservation laws that model the evolution of water saturation S (that is, the locally-averaged fraction of pore space occupied by water) have been, so far, unable to model gravity fingering successfully. The traditional model of unsaturated flow, known as Richards equation [12], is a mass balance equation in which the water flux is modeled by a straightforward extension of Darcy's law to unsaturated media. It accounts for gravity, capillarity, and the fact that the permeability to water is reduced because the porous medium is only partially saturated with water. It is well known that Richards equation leads to monotonic saturation profiles and cannot predict or simulate fingering under any conditions [13].

To remedy this behavior, several extensions to Richards equation have been proposed. These include a formulation with dynamic capillary pressure [14,13], designed to account for additional terms that arise from averaging of the microscopic multiphase flow equations. A related model [15] contains a hypodiffusive term, introduced to mimic the observed hold-back–pile-up effect, which gives rise to a saturation overshoot at the wetting front—a distinctive feature of fingered flows. Higher-order terms are required, however, to regularize the mathematical problem [16]. Here, we propose a physical mechanism and a subsequent continuum mathematical model that explain why gravity fingers occur during infiltration, and predict when and how they will grow.

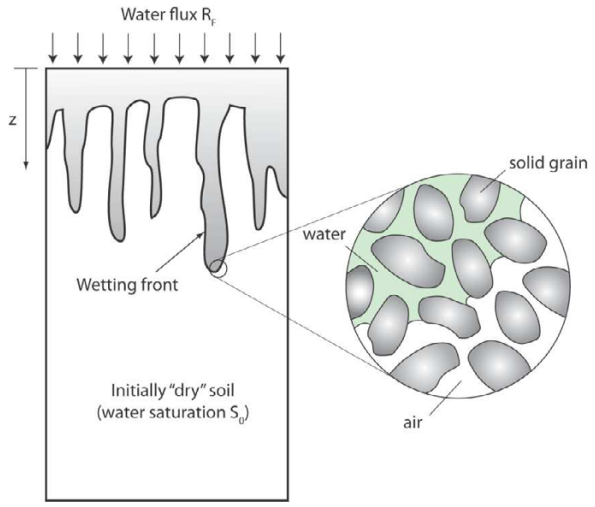

Fig. 3 Schematic of vertical infiltration of water into a porous medium. Initially, the soil is almost dry (water saturation S_0). A constant and uniformly distributed flux of water R_F (LT^{-1}) infiltrates into the soil. The flux of water is less than the hydraulic conductivity of the soil, K_s, so that the flux ratio $R_s = R_F/K_s < 1$. Macroscopically, a diffuse interface (the wetting front) moves downwards. This interface is often unstable and takes the form of long and narrow fingers that travel faster than the base of the wetting front (see, e.g., Fig. 2 in (glass1989b)). Microscopically, a sharp interface between water and air exists (see inset), which is locally governed by capillary effects.

Consider constant flux infiltration into a porous medium (Fig. 3). It is assumed that the initial water saturation S_0 is uniform, and that the infiltration rate R_F is uniformly distributed and constant in time. The z spatial coordinate points downwards, in the direction of gravity (acceleration g). The water density and dynamic viscosity are ρ and μ. The relevant (macroscopic) parameters concerning the porous medium are its intrinsic permeability k, and its porosity ϕ. The permeability of the medium is often expressed as a saturated hydraulic conductivity, $K_s = k\rho g/\mu$, which equals the gravity driven flux under full saturation. Hence, the infiltration rate R_F may be expressed as a flux ratio, $R_s = R_F/K_s$, with $R_s \in [0, 1]$. When this idealized flow scenario is simulated experimentally, the stability of the wetting front seems to be controlled by the flux ratio, initial saturation and material nonlinearity [15]. A saturation overshoot is observed at the tip of the fingers, which grow as traveling waves, advancing with constant velocity [17]. The formation of fingers appears as a winner-takes-all process, by which the fastest growing fingers in the initial unstable front channelize most of the infiltrating fluid and inhibit the growth of other incipient fingers [2,17]. The initial moisture content plays a critical role in the fingering instability: even relatively low saturations lead to a compact, downward moving wetting front [18]. Stable fronts are also observed in dry media when the infiltration rate is either very small or approaches the saturated conductivity. In general, larger infiltration rates produce faster, thicker fingers [2].

Our mathematical model for the water saturation S during infiltration, when expressed in dimensionless quantities, takes the form:

$$\frac{\partial S}{\partial t} + \nabla \cdot \left[k_r(S) \Big(\nabla z + Gr^{-1} \nabla J(S) + N\ell \nabla (\Delta S) \Big) \right] = 0. \tag{1}$$

where Gr and $N\ell$ are two dimensionless groups. Our model is similar to that describing the flow of thin films [19,20], and to phase-field models of epitaxial growth of surfaces and binary transitions [21,22]. The traditional Richards equation can be recovered by neglecting the nonlocal energy term in Eq. (1). We define the saturation-dependent relative permeability $k_r(S)$ and the dimensionless capillary pressure $J(S) = -\psi'(S)$. The functional forms of these constitutive relations are chosen to fit experimental data from quasi-static experiments. In the following, we adopt the van Genuchten–Mualem model [23],

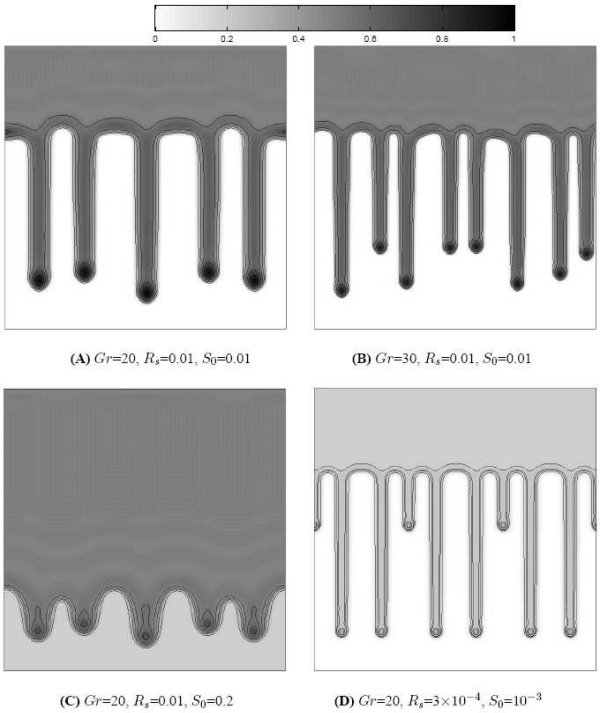

Fig. 4 Saturation maps from the numerical simulations of Eq. (1), for different values of the gravity number Gr, flux ratio R_s, and initial saturation S_0. Increasing the gravity number (**(A)** and **(B)**) changes the scale of the problem but not the nonlinear dynamics of the wetting front. Large initial saturations **(C)** lead to a compact invasion, and small flux ratios **(D)** produce thinner, slower fingers in sufficiently dry media. The flow dynamics and the distinctive saturation overshoot at the tip of the fingers, which behave as traveling waves, agree with experimental observations.

$$k_r(S) = \sqrt{S}\left[1 - \left(1 - S^{1/m}\right)^m\right]^2, \qquad J(S) = \left(S^{-1/m} - 1\right)^{1/n}, \tag{2}$$

where $m = 1 - 1/n$. This model introduces two intrinsic material parameters: α and n. The dimension of α is L^{-1}, and α^{-1} is approximately the capillary rise. The nonlinearity of the material is determined by n, which depends on how well-sorted the porous medium is. The gravity number Gr is defined as $Gr = \alpha L$, where L is an *arbitrary* length scale used to nondimensionalize the equations. The dependence of the capillary rise on the system parameters is given by the Leverett scaling $h_{\mathrm{cap}} \sim \alpha^{-1} \sim \gamma \cos\theta/(\rho g\sqrt{k/\phi})$, where γ is the surface tension between the fluids, and θ is the contact angle between the air–water interface and the solid surface [24].

Dimensional analysis leads to the scalings $Gr \sim L$ and $N\ell \sim L^{-3}$, which simply reflect that the solution should be independent of the choice of the reference lengthscale L. In principle, one might postulate the dependence of $N\ell$ on an additional intrinsic property of the system. Since the idea of a nonlocal interface is fundamentally a macroscopic construct, it is more rigorous to express $N\ell$ in terms of the already considered basic parameters, and thus arrive at the scaling $N\ell \sim Gr^{-3}$. The coefficient linking $N\ell$ and Gr^{-3} must be a constant, and simple analysis suggests that its magnitude is of the order of one. Therefore, we propose the relation

$$N\ell = Gr^{-3}. \tag{3}$$

As a consequence of Eq. (3), the gravity number Gr sets the intrinsic scale of the problem, and the proposed model contains a new term, but not a new independent parameter. The numerical solutions to Eq. (1) capture the

experimentally observed features of preferential flow and wetting front instability (Fig. 4). The most salient qualitative discrepancy between the numerical simulations and the experimental visualizations is the absence of meandering of the fingers, which is due to small heterogeneities and packing irregularities that always exist in the experiments and are not considered in the simulations. Our model permits investigation of the dependence of the flow characteristics with the various system parameters, and predicts the existence of a saturation ridge along the finger root front, which should be analyzed in future experiments.

The linear stability analysis of Eq. (1) provides further insight into the role of the system parameters on the dynamics of the flow. Stability refers here to the growth or decay of planar infinitesimal perturbations to the traveling wave solutions to Eq. (1). We distinguish between asymptotic (modal) and transient (non-modal) growth behavior, the latter arising from the non-normality of the linearized flow operator [25,20]. For each set of parameters, we determine the frequency $\omega_{\max}$ of the most unstable mode, as well as its associated asymptotic growth factor $\beta_{\max}$ and the transient growth behavior. Positive values of $\beta_{\max}$ or intense transient growth are indicative of an unstable wetting front, and their magnitudes correlate with the severity of fingering.

When the dimensionless groups Gr and $N\ell$ are considered independent, there is a narrow region in the parameter space Gr–$N\ell$ where $\omega_{\max}$ (Fig. 5(A)) and $\beta_{\max}$ (Fig. 5(B)) decay exponentially. This region of abrupt decay marks the effective transition from a compact infiltration front to fingering instability, and follows a straight line (in logarithmic scale) of slope -3. The specific location of the transition (not its slope) is determined by the system parameters R_s, S_0 and n. This critical region cannot be crossed when Gr moves along $N\ell = Gr^{-3}$, and therefore changes in the gravity number do not induce regime transition.

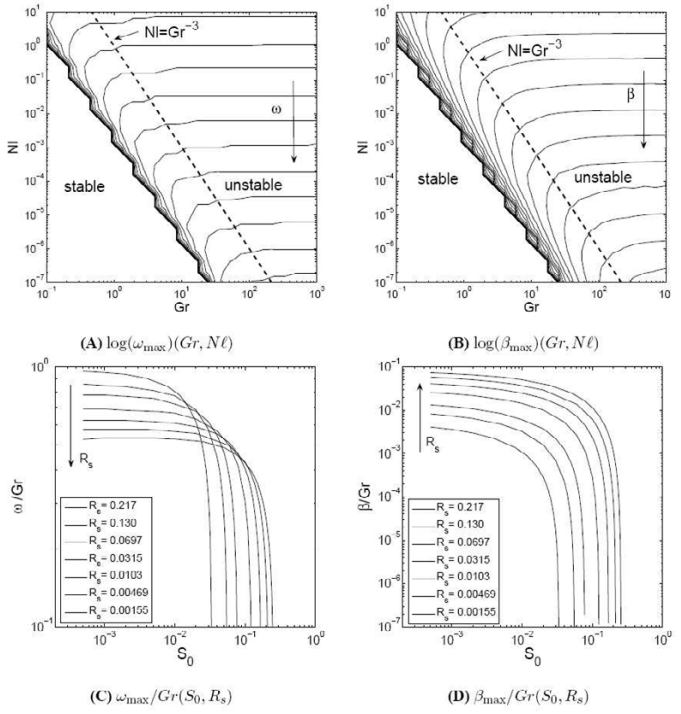

Fig. 5 Results of the linear stability analysis of Eq.(1). **(A)–(B)** Contours of the logarithm of the frequency $\omega_{\max}$ of the most unstable mode and its associated growth factor $\beta_{\max}$, as functions of the dimensionless groups Gr and $N\ell$. We set $R_s = 0.217$, $S_0 = 0.01$ and $n = 10$. A narrow region of exponential decay, along a straight line of slope -3, marks the effective transition from stable to unstable flow. The position of this transition region, not its slope, is determined by R_s, S_0 and n. Under the proposed scaling $N\ell = Gr^{-3}$, the transition region cannot be crossed by modifying Gr alone. **(C)** Exponential decay of the scale-invariant frequencies $\omega_{\max}/Gr$ with the initial saturation S_0. For a given S_0, the frequencies increase with decreasing R_s, up to a critical flux beyond which $\omega_{\max}/Gr$ decreases again. **(D)** Exponential decay of the scale□invariant growth factor $\beta_{\max}/Gr$ with the initial saturation S_0. Within the unsaturated regime, the growth factors

The stability analysis also reveals that, under the scaling $N\ell = Gr^{-3}$, $\omega_{\max}$ and $\beta_{\max}$ are linear functions of Gr. The scale-invariant frequencies and growth factors, $\omega_{\max}/Gr$ (Fig. 5(C)) and $\beta_{\max}/Gr$ (Fig. 5(D)), are indicative of the early dynamics of the perturbed flow and the properties of the emerging fingers. The onset of

preferential flow paths in the unstable wetting front is more intense for larger flux ratios and smaller initial saturations. For very dry media the size of the incipient fingers decreases with the flux ratio. In general, however, for each value of the initial saturation there is a critical flux ratio beyond which smaller fluxes lead to larger finger sizes (Fig. 5(C)). This nontrivial result shows that it is possible to observe both decrease and increase in finger size with decreasing R_s, depending on the particular values of R_s and S_0. The growth factor and frequency of the most unstable mode decay exponentially as the initial saturation is increased. This abrupt decay agrees with experimental observations, which have suggested the existence of critical values of S_0 for the suppression of the instability [18].

A linear stability analysis has applicability, strictly speaking, to incipient perturbation growth. The dominant role of the fastest growing fingers suggests, however, that the results of a modal analysis may correlate with the characteristics of the fully - developed fingers. Using dimensional analysis, and assuming that the finger properties can be determined from the basic system parameters and the dimensionless groups $\beta_{\max}$, $\omega_{\max}$ and Gr, we arrive at the following expressions for finger tip velocity v and finger width d:

$$v = \mathcal{C}_v \frac{K_s}{\phi} \frac{\beta_{\max}}{Gr}, \qquad d = \mathcal{C}_d \, \alpha^{-1} \left(\frac{\omega_{\max}}{Gr} \right)^{-1}, \tag{4}$$

where $\mathcal{C}_v$ and $\mathcal{C}_d$ are experimental constants. For initially dry media, the flux ratio has a relatively modest influence on $\omega_{\max}$ (Fig. 5(C)), and therefore Eq. (4) predicts that the finger width roughly scales like $d \sim h_{\text{cap}}$, which is consistent with experimental observations and scaling theories in porous media [26].

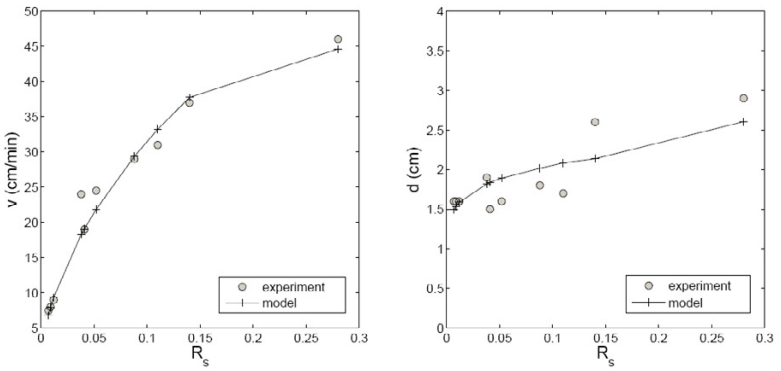

(A) Finger velocity **(B)** Finger width

Fig. 6 Average finger tip velocity **(A)** and finger width **(B)** versus flux ratio R_s. The circles are the experimental measurements of Glass et al. [2]. The crosses (joined by straight solid lines) are the values predicted by the linear stability analysis, together with Eq. (1). We set $S_0 = 0.0003$, $n = 10$, and a gravity number $Gr = 50$ based on the height of the experimental chamber. The constants in Eq. (4) are estimated as $\mathcal{C}_v = 6.8$ and $\mathcal{C}_d = 0.9$. The predictions based on the linear stability analysis reproduce the observed increase of finger velocity and finger size with the flux ratio.

To test these predictions, we compare the finger properties given by Eq. (4) with measurements from the experiments by Glass et al. [2]. They report experiments of infiltration into homogeneous, initially dry, coarse sands, for different flux ratios. Constant infiltration rates are achieved through the use of a two-layer configuration, with a tall, coarse-sand layer at the bottom of the chamber, and a thinner, less conductive, fine-sand layer on top. Comparison of the experimental and predicted finger characteristics (Fig. 6) suggests the choices $\mathcal{C}_v = 6.8$ and $\mathcal{C}_d = 0.9$. The results from the linear stability analysis, together with Eq. (4), not only reproduce the observed trends in finger velocity (Fig. 6(A)) and finger width (Fig. 6(B)), but also show good quantitative agreement with the experimental measurements.

3. Conclusions

The present study shows that gravity fingering in unsaturated flow can be explained, described and modeled by means of continuum balance laws. The success of this simple model to explain infiltration fingers suggests that similar continuum models, derived using the framework of phase-field modeling, may improve our ability to predict unstable multiphase flow in porous media.

Acknowledgements

We gratefully acknowledge funding for this research, provided by Eni under the Multiscale Reservoir Science project, and by the Winslow Career Development Chair.

References

1. D. E. Hill and J.-Y. Parlange, Soil Sci. Soc. Am. J. **36**, (1972) 397.
2. R. J. Glass, J.-Y. Parlange, and T. S. Steenhuis, Water Resour. Res. **25**, (1989) 1195.
3. D. Markewitz, E. A. Davidson, R. Figueiredo, R. L. Victoria, and A. V. Krusche, Nature **410**, (2001) 802.
4. C. Y. Wang, Chem. Rev. **104**, (2004) 4727.
5. P. G. Saffman and G. I. Taylor, Proc. R. Soc. Lond. **245**, (1958) 312.
6. R. L. Chuoke, P. van Meurs, and C. van der Poel, Petrol. Trans. Am. Inst. Min. Eng. **216**, (1959) 188.
7. J.-Y. Parlange and D. E. Hill, Soil Sci. **122**, (1976) 236.
8. D. A. Weitz, J. P. Stokes, R. C. Ball, and A. P. Kushnick, Phys. Rev. Lett. **59**, (1987) 2967.
9. D. A. DiCarlo and M. J. Blunt, Water Resour. Res. **36**, (2000) 2781.
10. B. Xu, Y. C. Yortsos, and D. Salin, Phys. Rev. E **57**, (1998) 739.
11. B. Berkowitz and R. P. Ewing, Rev. Geophys. **19**, (1998) 23.
12. L. A. Richards, Physics **1**, (1931) 318.
13. J. L. Nieber, R. Z. Dautov, A. G. Egorov, and A. Y. Sheshukov, Transp. Porous Media **58**, (2005) 147.
14. S. M. Hassanizadeh and W. G. Gray, Water Resour. Res. **29**, (1993) 3389.
15. M. Eliassi and R. J. Glass,Water Resour. Res. **38**, (2002) 1234.
16. D. A. DiCarlo, R. Juanes, T. LaForce, and T. P. Witelski, Water Resour. Res. **44**, (2008) W02406.
17. J. S. Selker, J.-Y. Parlange, and T. Steenhuis,Water Resour. Res. **28**, (1992) 2523.
18. T. X. Lu, J. W. Biggar, and D. R. Nielsen, Water Resour. Res. **30**, (1994) 3283.
19. H. E. Huppert, Nature **300**, (1982) 427.
20. A. L. Bertozzi and M. P. Brenner, Phys. Fluids **9**, (1997) 530.
21. M. Dub´e, M. Rost, K. R. Elder, M. Alava, S. Majaniemi, and T. Ala-Nissila, Phys. Rev. Lett. **83**, (1999) 1628.
22. H. Emmerich, Adv. Phys. **57**, (2008) 1.
23. M. T. van Genuchten, Soil Sci. Soc. Am. J. **44**, (1980) 892.
24. P. G. de Gennes, Rev. Mod. Phys. **57**, (1985) 827.
25. L. N. Trefethen, A. E. Trefethen, S. C. Reddy, and T. A. Driscoll, Science **261**, (1993) 578.
26. J. S. Selker and M. H. Schroth, Water Resour. Res. **34**, (1998) 1935.